

Original Article

## Investigation of the mechanism of poly (ADP-ribose) polymerase (PARP) in elderly mouse myocardial ischemia-reperfusion injury

Xueyuan Wang<sup>1</sup>, Xiaocan Yan<sup>2</sup>, Yin Xi<sup>1</sup>, Jie Hao<sup>1</sup>, Jinming Liu<sup>1,\*</sup><sup>1</sup> Department of Cardiology, The Second Hospital of Hebei Medical University, Shijiazhuang, China<sup>2</sup> Department of General Surgery, The Second Hospital of Hebei Medical University, Shijiazhuang, China

### Article Info

### Abstract



#### Article history:

Received: March 01, 2024

Accepted: June 29, 2024

Published: August 31, 2024

Use your device to scan and read the article online



This study investigated the role of Poly (ADP-ribose) Polymerase (PARP) in myocardial ischemia-reperfusion injury (MIRI) in elderly mice. It involves 30 elderly male KM mice divided into three groups: Sham, MIRI, and DPQ, where the MIRI and DPQ groups undergo myocardial ischemia-reperfusion with the DPQ group also receiving DPQ for PARP-1 inhibition. Over three weeks, assessments include histological analysis of myocardial lesions, left ventricular ejection fraction (LVEF) measurements, and evaluations of serum cardiac enzymes and inflammatory markers. This approach aims to understand the protective effects of DPQ in MIRI, focusing on its impact on cardiac health and inflammation via the JAK2/STAT3 pathway. The findings suggest that PARP activation exacerbates cardiac dysfunction and inflammation in MIRI by possibly modulating the JAK2/STAT3 signaling pathway. Inhibition of PARP-1 with DPQ mitigates these effects, as indicated by reduced myocardial lesions and inflammatory infiltration, improved LVEF, and altered levels of inflammatory markers and signaling molecules. However, the differences in STAT3 and p-STAT3 protein expression between the DPQ and MIRI groups were not statistically significant, suggesting that while PARP inhibition affects many aspects of MIRI pathology, its impact on the JAK2/STAT3 pathway may not fully explain the observed benefits. This study contributes to our understanding of the complex mechanisms underlying myocardial ischemia-reperfusion injury, particularly in the context of aging. It highlights the potential of PARP inhibition as a therapeutic strategy to attenuate cardiac dysfunction and inflammation in MIRI, though further research is necessary to fully elucidate the underlying molecular pathways and to explore the clinical relevance of these findings in humans.

**Keywords:** PARP, MIRI, DPQ, JAK2/STAT3 signaling pathway, KM mice.

### 1. Introduction

Myocardial Ischemia-Reperfusion Injury (MIRI) is a severe complication observed in patients with myocardial infarction, characterized by arrhythmias, increased infarct size, decreased cardiac ejection fraction, and cardiac cell death during the process of blood flow reconstruction [1]. With the increasing aging population, the incidence and mortality rates of acute myocardial infarction are on the rise. Clinical interventions often involve percutaneous coronary intervention [2]. While this method successfully induces early revascularization/reperfusion, it may lead to intensified cardiac damage, ultimately causing MIRI. This results in the progression of the disease, worsening of the patient's condition, and, in severe cases, death. Therefore, finding an effective treatment for acute myocardial infarction that also reduces the occurrence of MIRI is crucial [2, 3]. However, the unclear pathogenesis of MIRI poses a significant challenge. Poly (ADP-ribose) Polymerase (PARP) is a crucial enzyme involved in repairing DNA damage in cellular tissues, widely present in the nuclei of most eukaryotic cells [4]. Research indicates a close association between PARP and the occurrence of MIRI. Ex-

cessive reactive oxygen species (ROS) generated during oxidative stress can cause substantial DNA chain damage, leading to the overactivation of PARP. PARP plays a pivotal role in the occurrence of MIRI [5]. The Janus kinase 2 (JAK2)/Signal Transducer and Activator of Transcription 3 (STAT3) signaling pathway is a classical pathway mediating inflammatory responses, and promoting the expression of anti-inflammatory factors [3, 6]. Studies have shown that inhibiting the expression of PARP-1 can alleviate MIRI-induced cardiac damage, and the regulation of the JAK2/STAT3 signaling pathway can protect against cardiac injury in MIRI rats [7]. PARP-1 inhibitor (DPQ) can suppress the expression of PARP-1 in the body. Research suggests that PARP-1 inhibitors play a role in regulating oxidative stress reactions and also have a modulatory effect on inflammatory factors [7, 8]. Therefore, this study aims to observe the impact of PARP regulation of the signaling pathway on elderly MIRI mice, exploring the potential mechanism of PARP in elderly MIRI mice [7, 9]. This research aims to provide a theoretical basis for the prevention and treatment of clinical MIRI.

\* Corresponding author.

E-mail address: [27400103@hebmu.edu.cn](mailto:27400103@hebmu.edu.cn) (Jinming Liu).Doi: <http://dx.doi.org/10.14715/cmb/2024.70.8.13>

## 2. Materials and Methods

### 2.1. Experimental animals

A total of 30 SPF-grade healthy elderly male KM mice (>72 weeks old), with a body weight range of 18-22 g and an average body weight of (20±1) g, were obtained from Jinan Pengyue Experimental Animal Breeding Co., Ltd. The mice were provided with ad libitum access to food and water, subjected to a 12-hour light-dark cycle, and maintained under standard conditions with a room temperature of (25±2)°C and 50%±5% humidity. Ethical approval for this experiment was obtained from the Animal Experimental Ethics Committee of Hebei Medical University.

### 2.2. Establishment and grouping of MIRI Model

Thirty SPF-grade healthy elderly male KM mice were randomly divided into three groups after one week of adaptive feeding: Sham group, Myocardial Ischemia-Reperfusion Injury (MIRI) group, and Poly (ADP-ribose) Polymerase 1 (PARP-1) inhibition group (DPQ group), with 10 mice in each group. The MIRI model was established in reference to literature [9], using the left anterior descending coronary artery ligation method. After abdominal injection with 10% chloral hydrate for anesthesia, the mice were subjected to left anterior descending coronary artery ligation. The success of ligation was confirmed by changes such as immediate blanching or cyanosis of the left ventricular free wall and ST-segment elevation in the electrocardiogram. The ligature was loosened after 50 minutes of ischemia to restore blood supply, achieving 120 minutes of reperfusion. Successful establishment of the MIRI model was confirmed by a decrease in the ST-segment elevation by more than half. In the Sham group, mice underwent thoracotomy to expose the heart, and a suture was passed without ligation. The remaining procedures were the same as in the model group. In the DPQ group, 2.5 mg/(kg·d) DPQ was injected into the abdominal cavity after 120 minutes of reperfusion. The model and sham groups received an equivalent amount of normal saline by abdominal injection. Continuous drug intervention was performed for 3 weeks.

### 2.3. Main Reagents and instruments

Reagents: DPQ (Beijing Solaibao Biotechnology Co., Ltd., CLP0797, Beijing, China); IL-6 ELISA kit (Nanjing Jiancheng Bioengineering Institute, Nanjing, China); IL-10 ELISA kit (Nanjing Jiancheng Bioengineering Institute, Nanjing, China); AST, LDH, CK-MB (Shenzhen Maire Biomedical Electronics Co., Ltd., Shenzhen, China); PARP antibody (ABmart, T40050, Shanghai, China); JAK2, p-JAK2, STAT3, p-STAT3 antibodies (Shenyang Wanlei Biotechnology Co., Ltd., WL02188, WL02997, WL01836, WLP2412, Shenyang, China); GAPDH (ABmart, M20006, Shanghai, China); Horseradish peroxidase-labeled goat anti-rabbit IgG (Beijing Zhongshan Jin Qiao Biological Co., Ltd., AS014, Beijing, China); 4% paraformaldehyde fixative (Biosharp); BCA Protein Assay Kit (ThermoFisher, 23227, Waltham, MA, USA); RIPA lysis buffer (Shanghai Biyuntian Biotechnology Co., Ltd., P0013C, Shanghai, China); Protein marker (Shanghai Tianneng Technology Co., Ltd., 180-6003, Shanghai, China).

Instruments: Selectra E fully automated biochemical analyzer (Shanghai Yuyan Scientific Instruments Co., Ltd., Shanghai, China); MyLab Doppler ultrasound ma-

chine (ESAOTE, Italy); High-speed tabletop refrigerated centrifuge (Anhui Jiawen Instrument Equipment Co., Ltd., JW-3021HR, Hefei, China); Microplate reader (Thermo-Lab System); Paraffin slicer (Leica, Wetzlar, Germany); Optical microscope (Olympus, Tokyo, Japan); Grinding machine (Shanghai Jingxin Industrial Development Co., Ltd., Shanghai, China); Gel imaging system (Protein-Simple, FlourChem FC30, St. Louis, MO, USA).

### 2.4. Experimental Methods

#### 2.4.1. Histological staining of mouse cardiac tissues around the injury site with HE

After euthanizing the mice by decapitation, the cardiac tissues surrounding the injury site were dissected and immersed in 4% paraformaldehyde for 24 hours to fix the tissues and induce protein denaturation. The remaining tissues were stored at -80°C. The fixed tissues were processed through dehydration, transparency, embedding, and sectioning to create paraffin sections with a thickness of approximately 5 µm. The sections were floated in a 40°C water bath and baked at 60°C for 1 hour. Standard deparaffinization was performed twice with xylene for 5 minutes each, followed by dehydration in a series of ethanol concentrations (100%, 95%, 80%, and 70%) for 15 minutes each. Subsequently, the sections were rinsed with distilled water for 5 minutes (three times). Staining was carried out using hematoxylin for 5 minutes, and staining time was adjusted based on actual staining conditions. After water rinsing, 5% acetic acid differentiation was performed for 1 minute, followed by water rinsing. Eosin staining was performed for 1 minute, and staining time was adjusted based on actual conditions. The sections were dehydrated using 70%, 80%, 90%, and 100% ethanol for 10 seconds each, followed by 1 minute in xylene. The sections were then air-dried overnight in a fume hood, covered with neutral resin, and sealed. The morphological characteristics of cardiac tissues around the injury site in the three groups of mice were observed under a microscope.

#### 2.4.2. Measurement of Left Ventricular Ejection Fraction (LVEF) in mice

Using the MyLab Doppler ultrasound machine, cardiac function was assessed 24 hours before modeling and 3 weeks after modeling. The left ventricular ejection fraction (LVEF) was measured by placing the mice in a supine position, shaving the chest area, applying ultrasound coupling agent, and positioning the ultrasound probe on the left side of the sternum to obtain M-mode ultrasound for LVEF measurement.

#### 2.4.3. Measurement of serum AST, LDH, and CK-MB in mice

After completion of cardiac function ultrasound examination, the mice were anesthetized, blood was collected by extracting the eyeballs, and the mice were euthanized by decapitation. The upper layer of serum was obtained by centrifugation, and AST, LDH, and CK-MB were measured using the Selectra E fully automated biochemical analyzer.

#### 2.4.4. Enzyme-Linked Immunosorbent Assay (ELISA) for detecting mouse cardiac TNF-α, IL-6, and IL-10 levels

After euthanasia, mouse heart tissues were collected,

part of which was washed in 0.9% sodium chloride solution, and the remaining part was stored at  $-80^{\circ}\text{C}$ . Approximately 100 mg of cleaned tissue around the injury site was taken and homogenized in PBS solution at a ratio of 1:9. The homogenate was centrifuged at 12,000 rpm for 15 minutes at  $4^{\circ}\text{C}$ , and the supernatant was collected and sealed for freezing at  $-80^{\circ}\text{C}$ . TNF- $\alpha$ , IL-6, and IL-10 levels were determined according to the instructions of the ELISA kits. The specific steps were as follows: Samples, wells, and standards were allowed to stand at room temperature for 30 minutes. After washing the microplate with 500  $\mu\text{L}$  of Wash Buffer, the residual liquid in the well was removed with absorbent paper. A total of 100  $\mu\text{L}$  of Sample Diluent was added to the standard microplate wells and the secondary wells. Graded dilutions were performed five times, and equal amounts of Sample Diluent were added to the blank reference wells. Then, 50  $\mu\text{L}$  of Sample Diluent sample dilution was added to the sample wells and secondary wells, respectively, and covered. The microplate was shaken using a plate shaker at 400 rpm for 2 hours. After removing the cover, the liquid in the well was discarded. The microplate was washed three times with TBST, and 100  $\mu\text{L}$  of antibiotic-protein A-HRP was added. The plate was covered again, shaken slowly for 1 hour at room temperature, and the cover was removed, followed by discarding the liquid in the well. The microplate was washed again with TBST for 6 minutes  $\times$  5 times. Then, 100  $\mu\text{L}$  of TMB was added, and incubation was carried out for 10 minutes. After adding 100  $\mu\text{L}$  of stop solution to terminate the enzyme reaction, the absorbance was measured using a microplate reader at a reference wavelength of 450 nm. Standard curves were plotted, and the levels of each inflammatory factor were calculated.

#### 2.4.5. Western Blot for detecting protein expression of PARP, JAK2, p-JAK2, STAT3, and p-STAT3

About 100mg of mouse heart tissue samples around the injury site, stored at  $-80^{\circ}\text{C}$ , were taken and thoroughly ground, followed by adding 500  $\mu\text{L}$  of RIPA lysis buffer for homogenization treatment for 3 minutes. The mixture was then lysed at  $4^{\circ}\text{C}$  for 30 minutes and centrifuged at 12,000 rpm for 10 minutes at  $4^{\circ}\text{C}$ . The supernatant was collected. The protein content of each group was determined using the BCA assay kit. After preparing the concentration of concentrated gel and separating gel, the appropriate amount of electrophoresis buffer was added to the electrophoresis tank. The sample was loaded with 1  $\mu\text{L}$ , the marker with 0.5  $\mu\text{L}$ , and electrophoresis was carried out at a constant voltage of 80 V for 30 minutes, followed by increasing the voltage to 120 V with a set electrophoresis time based on protein size. Before transferring, the PVDF membrane was marked and treated with methanol for 5 seconds. After soaking in the buffer for 20 minutes, the gel containing the target band was cut and placed on filter paper. The PVDF membrane was covered, the filter paper was placed on top, and the transfer clamp was tightly clamped before transferring to the electrophoresis cell. After the transfer was completed, the PVDF membrane was washed with TBST for 5 minutes, followed by adding blocking solution and incubating slowly on a shaker at room temperature for 2.5 hours. After blocking, the PVDF membrane was washed with TBST for 6 minutes  $\times$  5 times. The PVDF membrane was then added to the diluted antibodies [PARP (1:800), JAK2 (1:1000), p-JAK2 (1:800), STAT3

(1:750), p-STAT3 (1:600), GAPDH (1:5000)] and incubated overnight at  $4^{\circ}\text{C}$ . The membrane was washed with TBST, and the secondary antibody (1:5000) was added, followed by incubation at room temperature for 2 hours. The membrane was washed with TBST for 6 minutes  $\times$  5 times. Protein expression was analyzed using a gel imaging analysis system after developing with the substrate.

#### 2.5. Statistical analysis

Statistical analysis of the data in this study was performed using Statistical Product and Service Solutions (SPSS) 22.0 software (IBM, Armonk, NY, USA). Measurement data are expressed as mean  $\pm$  standard deviation ( $\bar{x}\pm s$ ). One-way analysis of variance (ANOVA) was used for comparisons among the three groups, and LSD-t test was used for pairwise comparisons between groups. Count data are expressed as frequencies and were analyzed using the chi-square test. A significance level of  $P < 0.05$  was considered statistically significant.

### 3. Results

#### 3.1. Comparison of HE staining of mouse cardiac tissues around the injury site

After 3 weeks of intervention, HE staining of cardiac tissue sections around the injury site was performed in the three groups of mice. In the Sham group, the cardiac tissue structure was clear, complete, and uniformly stained, with orderly arrangement of myocardial fibers. In comparison to the Sham group, the cardiac tissues of mice in the MIRI group were significantly damaged, with loose and disordered arrangement of myocardial fibers, vacuolar degeneration, partial nuclear condensation, fragmentation, and infiltration of a large number of inflammatory cells. In the DPQ group, the degree of lesion was reduced compared to the MIRI group, the arrangement of myocardial fibers tended to be orderly, tissue structure density increased, and inflammatory cell infiltration decreased, as shown in Figure 1.

#### 3.2. Comparison of Left Ventricular Ejection Fraction (LVEF) in mice

After 3 weeks of intervention, compared to the same group 24 hours before modeling, LVEF in the MIRI group and DPQ group significantly decreased, with statistical significance ( $P < 0.05$ ). LVEF in the DPQ group was significantly higher than that in the MIRI group but lower than that in the Sham group, with statistical significance ( $P < 0.05$ ). Refer to Table 1.

#### 3.3. Comparison of mouse serum AST, LDH, and CK-MB levels

After 3 weeks of intervention, the levels of AST, LDH,

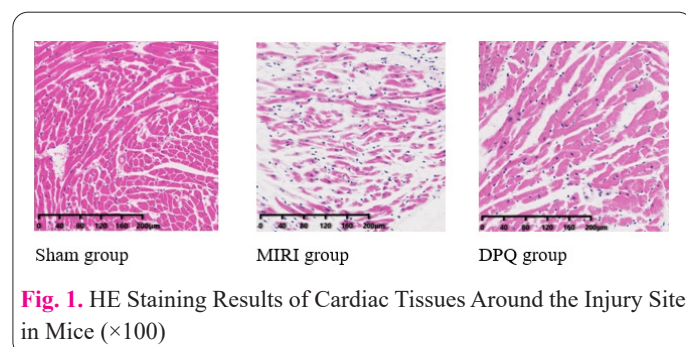


**Fig. 1.** HE Staining Results of Cardiac Tissues Around the Injury Site in Mice ( $\times 100$ )



**Table 1.** Comparison of Left Ventricular Ejection Fraction (LVEF) in Mice in Each Group (n=10, x±s, %).

Group	Before Model 24 h	After 3 weeks of successful modeling
Sham group	46.54±2.01	48.45±2.11
MIRI group	45.35±1.99	27.15±3.05*#
DPQ group	45.86±2.06	34.57±1.84*#Δ

Note: Compared with the pre-modeling 24h, \*P < 0.05; compared with the Sham group, #P < 0.05; compared with the MIRI group, ΔP < 0.05.

and CK-MB in the MIRI group were significantly higher than those in the Sham group, with statistical significance (P < 0.05). The levels of AST, LDH, and CK-MB in the DPQ group were significantly lower than those in the MIRI group but higher than those in the Sham group, with statistical significance (P < 0.05). See Table 2.

### 3.4. Comparison of mouse cardiac inflammatory responses by ELISA

After 3 weeks of intervention, the levels of TNF-α and IL-6 in the MIRI group were significantly higher than those in the Sham group, while the level of IL-10 was significantly lower than that in the Sham group, with statistical significance (P < 0.05). In the DPQ group, the levels of TNF-α and IL-6 were significantly lower than those in the MIRI group but higher than those in the Sham group. The IL-10 level was higher than that in the MIRI group but lower than that in the Sham group, and the differences were statistically significant (P < 0.05). See Table 3.

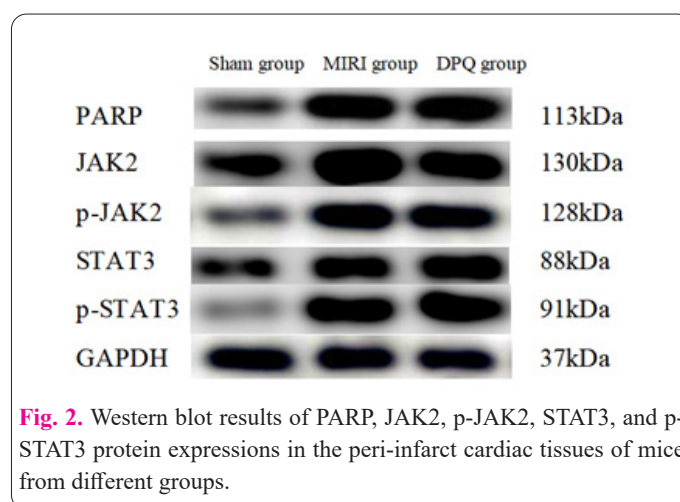
### 3.5. Comparison of PARP, JAK2, p-JAK2, STAT3, and p-STAT3 protein expression by Western blot after 3 weeks of intervention

After 3 weeks of intervention, the protein expression levels of PARP, JAK2, p-JAK2, STAT3, and p-STAT3 in

the MIRI group were significantly higher than those in the Sham group, with statistical significance (P < 0.05). The protein expression levels of PARP, JAK2, and p-JAK2 in the DPQ group were lower than those in the MIRI group, showing statistical significance (P < 0.05), while the protein expression levels of STAT3 and p-STAT3 were lower than those in the MIRI group but did not reach statistical significance (P > 0.05). See Figure 2 and Table 4.

## 4. Discussion

MIRI is a common cardiovascular disease that occurs during percutaneous coronary intervention or coronary artery bypass graft surgery [10]. Clinical manifestations include symptoms such as palpitations, shortness of breath, chest pain, and arrhythmias, predominantly affecting the elderly population [11]. Severe cases can lead to shock and even death. Poly (ADP-ribose) polymerase (PARP), as a DNA repair enzyme, is closely related to the occurrence and development of MIRI [12]. When tissues and cells are damaged, PARP increases significantly, and pro-

**Table 2.** Comparison of serum AST, LDH, and CK-MB levels in different groups of mice (n=10, x±s, U/L).

Group	AST	LDH	CK-MB
Sham group	105.25±11.56	4026.15±617.23	496.21±74.26
MIRI group	330.11±28.02*	5768.85±861.65*	689.85±99.89*
DPQ group	218.57±31.42*#	4998.84±751.15*#	545.25±77.21#

Note: \*P < 0.05 compared to the Sham group; #P < 0.05 compared to the MIRI group.

**Table 3.** Comparison of TNF-α, IL-6, and IL-10 levels in mouse cardiac tissues among different groups (n=10, x±s, pg/mL).

Group	TNF-α	IL-6	IL-10
Sham group	31.85±3.06	37.15±3.24	312.51±10.15
MIRI group	77.89±2.39*	79.11±2.42*	199.26±5.26*
DPQ group	48.01±3.35*#	48.13±3.89*#	216.58±6.95*

Note: \*P < 0.05 compared with the Sham group; #P < 0.05 compared with the MIRI group.

**Table 4.** Comparison of protein levels of PARP, JAK2, p-JAK2, STAT3, and p-STAT3 in cardiac tissues among different groups of mice (n=10, x±s).

Group	PARP/GAPDH	JAK2/GAPDH	p-JAK2/GAPDH	STAT3/GAPDH	p-STAT3/GAPDH
Sham group	0.61±0.03	0.36±0.01	0.28±0.03	0.66±0.02	0.49±0.03
MIRI group	1.24±0.08*	1.51±0.09*	1.29±0.07*	0.95±0.06*	1.07±0.08*
DPQ group	0.85±0.04*#	1.23±0.07*#	0.58±0.04*#	0.91±0.07*	1.02±0.01*

Group: Compared with the Sham group, \*P < 0.05; compared with the MIRI group, #P < 0.05.

longed stress leads to excessive PARP activation, resulting in adverse effects [13].

The mechanism by which PARP induces MIRI is currently unclear. This study investigated the role of PARP in aged MIRI mice, and the results showed that after 3 weeks of intervention, compared with the Sham group, the MIRI group exhibited severe lesions in the myocardium around the injury site, with disordered arrangement of myocardial cells, partial cell degeneration, necrosis, and extensive infiltration of inflammatory cells. DPQ intervention significantly improved the degree of lesions, indicating that inhibiting PARP expression can reduce myocardial damage in MIRI mice and exert a certain cardioprotective effect. This finding is supported by a study that found that downregulating PARP-1 expression can inhibit cardiac inflammation and cell apoptosis in myocardial infarction rats, thereby improving cardiac dysfunction [14].

After 3 weeks of intervention, the LVEF of the MIRI group decreased, and the levels of serum AST, LDH, and CK-MB increased, indicating a decline in cardiac function in MIRI mice. ELISA results showed that the levels of TNF- $\alpha$  and IL-6 in the hearts of MIRI mice increased significantly, while the level of IL-10 decreased. After DPQ intervention, the expression trends of these indicators were opposite to those in the MIRI group, suggesting that MIRI mice experienced an inflammatory response, and inhibiting excessive PARP expression could improve the body's inflammatory response.

The signaling pathway is a recently discovered signal transduction pathway shared by various cytokines [15, 16]. It plays an important role in stress response, regulation of inflammation, immunity, and cell apoptosis, and is closely related to the development of MIRI in mice. Studies have pointed out that inhibiting the JAK2/STAT3 pathway with paeoniflorin can suppress inflammation in the retinal cells of diabetic rats [15, 17]. This study used Western blotting to detect the expression of target proteins and found that the levels of PARP, JAK2, p-JAK2, STAT3, and p-STAT3 proteins were significantly higher in the MIRI group than in the Sham group, suggesting that PARP may promote the occurrence and development of MIRI through the regulation of the JAK2/STAT3 signaling pathway. After 3 weeks of DPQ intervention, the levels of PARP, JAK2, and p-JAK2 proteins in the DPQ group were lower than those in the MIRI group, with statistical significance, while the levels of STAT3 and p-STAT3 proteins were lower but not statistically significant. This may be related to DPQ inhibiting PARP expression and thereby affecting the JAK2/STAT3 pathway.

Some scholars have found that the traditional Chinese medicine formula "Right Returning Pill" can inhibit the Leptin/JAK2/STAT3 signaling pathway and improve inflammatory reactions in COPD rats [18], supporting the results of this study. It is also found that using granulocyte colony-stimulating factors can inhibit PARP activity and the JAK2/STAT3 signaling pathway, regulate the expression of downstream inflammatory factors, promote the recovery of mouse cardiac function, and alleviate myocardial cell apoptosis [19, 20]. This is consistent with the results of this study, where the DPQ group showed a decrease in inflammatory indicators and an improvement in the degree of lesions when PARP expression decreased compared to the MIRI group. Another study also found that effectively inhibiting early PARP-1 expression in cardiac MIRI can

alleviate reperfusion myocardial injury and protect the heart, supporting the conclusions of this study [21].

In summary, the mechanism by which PARP regulates aged MIRI mice may be related to its regulation of the JAK2/STAT3 signaling pathway. When the expression level of PARP is elevated in MIRI mice, cardiac function damage and myocardial inflammatory reactions exacerbate. However, after inhibiting PARP expression, the cardiac function and inflammatory reactions of mice in the DPQ group are significantly improved. This may provide a reference for the study and clinical application of the anti-inflammatory mechanism of PARP in aged MIRI patients. The shortcomings of this study include not exploring the specific mechanism of action of a specific protein in the PARP family and whether PARP can exert myocardial protective effects through other signaling pathways, which require further investigation.

#### Conflict of interests

The author has no conflicts with any step of the article preparation.

#### Consent for publications

The author read and approved the final manuscript for publication.

#### Ethics approval and consent to participate

This study was approved by the Animal Ethics Committee of Hebei Medical University Animal Center.

#### Informed consent

The authors declare that no patients were used in this study.

#### Availability of data and material

The data that support the findings of this study are available from the corresponding author upon reasonable request.

#### Authors' contributions

Xueyuan Wang and Jinming Liu designed the study and performed the experiments, Xiaocan Yan and Yin Xi collected the data, Xiaocan Yan, Yin Xi and Jie Hao analyzed the data, Xueyuan Wang and Jinming Liu prepared the manuscript. All authors read and approved the final manuscript.

#### Funding

None.

#### References

1. Algoet M, Janssens S, Himmelreich U, Gsell W, Pusovnik M, Van den Eynde J et al (2023) Myocardial ischemia-reperfusion injury and the influence of inflammation. *Trends Cardiovas Med* 33:357-366. doi: 10.1016/j.tcm.2022.02.005
2. Chen M, Zhong G, Liu M, He H, Zhou J, Chen J et al (2023) Integrating network analysis and experimental validation to reveal the mitophagy-associated mechanism of Yiqi Huoxue (YQHX) prescription in the treatment of myocardial ischemia/reperfusion injury. *Pharmacol Res* 189:106682. doi: 10.1016/j.phrs.2023.106682
3. Fan Q, Tao R, Zhang H, Xie H, Lu L, Wang T et al (2019) Dectin-1 Contributes to Myocardial Ischemia/Reperfusion Injury by Regulating Macrophage Polarization and Neutrophil Infiltration. *Circulation* 139:663-678. doi: 10.1161/CIRCULATIONAHA.118.036044

4. Galeone A, Grano M, Brunetti G (2023) Tumor Necrosis Factor Family Members and Myocardial Ischemia-Reperfusion Injury: State of the Art and Therapeutic Implications. *Int J Mol Sci* 24:4606. doi: 10.3390/ijms24054606
5. Chen M, Li X, Yang H, Tang J, Zhou S (2020) Hype or hope: Vagus nerve stimulation against acute myocardial ischemia-reperfusion injury. *Trends Cardiovas Med* 30:481-488. doi: 10.1016/j.tcm.2019.10.011
6. Chen J, Luo Y, Wang S, Zhu H, Li D (2019) Roles and mechanisms of SUMOylation on key proteins in myocardial ischemia/reperfusion injury. *J Mol Cell Cardiol* 134:154-164. doi: 10.1016/j.yjmcc.2019.07.009
7. Reda E, Hassaneen S, El-Abhar HS (2018) Novel Trajectories of Bromocriptine Antidiabetic Action: Leptin-IL-6/ JAK2/p-STAT3/ SOCS3, p-IR/p-AKT/GLUT4, PPAR-gamma/Adiponectin, Nrf2/ PARP-1, and GLP-1. *Front Pharmacol* 9:771. doi: 10.3389/fphar.2018.00771
8. Laspata N, Kaur P, Mersaoui SY, Muoio D, Liu ZS, Bannister MH et al (2023) PARP1 associates with R-loops to promote their resolution and genome stability. *Nucleic Acids Res* 51:2215-2237. doi: 10.1093/nar/gkad066
9. Guo S, Zhang S, Zhuang Y, Xie F, Wang R, Kong X et al (2023) Muscle PARP1 inhibition extends lifespan through AMPKalpha PARylation and activation in *Drosophila*. *P Natl Acad Sci Usa* 120:e2081110176. doi: 10.1073/pnas.2213857120
10. Li T, Tan Y, Ouyang S, He J, Liu L (2022) Resveratrol protects against myocardial ischemia-reperfusion injury via attenuating ferroptosis. *Gene* 808:145968. doi: 10.1016/j.gene.2021.145968
11. Fu DG (2015) Cardiac Arrhythmias: Diagnosis, Symptoms, and Treatments. *Cell Biochem Biophys* 73:291-296. doi: 10.1007/s12013-015-0626-4
12. Wang Y, Luo W, Wang Y (2019) PARP-1 and its associated nucleases in DNA damage response. *DNA Repair* 81:102651. doi: 10.1016/j.dnarep.2019.102651
13. Lin WL, Chen JK, Wen X, He W, Zarceno GA, Chen Y et al (2022) DDX18 prevents R-loop-induced DNA damage and genome instability via PARP-1. *Cell Rep* 40:111089. doi: 10.1016/j.celrep.2022.111089
14. Wang Z, Lee SJ, Cheng HJ, Yoo JJ, Atala A (2018) 3D bioprinted functional and contractile cardiac tissue constructs. *Acta Biomater* 70:48-56. doi: 10.1016/j.actbio.2018.02.007
15. Zhong Y, Gu L, Ye Y, Zhu H, Pu B, Wang J et al (2022) JAK2/STAT3 Axis Intermediates Microglia/Macrophage Polarization During Cerebral Ischemia/Reperfusion Injury. *Neuroscience* 496:119-128. doi: 10.1016/j.neuroscience.2022.05.016
16. Halmosi R, Deres L, Gal R, Eros K, Sumegi B, Toth K (2016) PARP inhibition and postinfarction myocardial remodeling. *Int J Cardiol* 217 Suppl:S52-S59. doi: 10.1016/j.ijcard.2016.06.223
17. Zhu H, Jian Z, Zhong Y, Ye Y, Zhang Y, Hu X et al (2021) Janus Kinase Inhibition Ameliorates Ischemic Stroke Injury and Neuroinflammation Through Reducing NLRP3 Inflammasome Activation via JAK2/STAT3 Pathway Inhibition. *Front Immunol* 12:714943. doi: 10.3389/fimmu.2021.714943
18. Hou Y, Wang K, Wan W, Cheng Y, Pu X, Ye X (2018) Resveratrol provides neuroprotection by regulating the JAK2/STAT3/PI3K/AKT/mTOR pathway after stroke in rats. *Genes Dis* 5:245-255. doi: 10.1016/j.gendis.2018.06.001
19. Zhang W, Xu M, Chen F, Su Y, Yu M, Xing L et al (2023) Targeting the JAK2-STAT3 pathway to inhibit cGAS-STING activation improves neuronal senescence after ischemic stroke. *Exp Neurol* 368:114474. doi: 10.1016/j.expneurol.2023.114474
20. Lv S, Ju C, Peng J, Liang M, Zhu F, Wang C et al (2020) 25-Hydroxycholesterol protects against myocardial ischemia-reperfusion injury via inhibiting PARP activity. *Int J Biol Sci* 16:298-308. doi: 10.7150/ijbs.35075
21. Tang Q, Xing C, Li M, Jia Q, Bo C, Zhang Z (2022) Pirfenidone ameliorates pulmonary inflammation and fibrosis in a rat silicosis model by inhibiting macrophage polarization and JAK2/STAT3 signaling pathways. *Ecotox Environ Safe* 244:114066. doi: 10.1016/j.ecoenv.2022.114066